Computational Methods for Materials Science

Lab Report

Elliot Perviz*

Department of Control Engineering, Czech Technical University in Prague

E-mail: perviell@fel.cvut.cz

Abstract

To demonstrate the functionality and scientific information that can be extracted from Molecular Dynamics (MD) and Quantum Mechanical (QM) materials science simulations, two separate investigations are performed. First, the thermal conductivity of a Single Wall Carbon Nanotube (SWCNT) is determined over a temperature range between 100-500 K through a MD simulation. It is found that there is a linear relationship between thermal conductivity and temperature with a gradient of 6.40 W/mK, in disagreement with previously published literature. Second, the electronic density of states (DOS) and band structure of $MoSe_2$ and WSe_2 are studied using QM simulations. Each material is found to be a direct band gap semiconductor with respective band gap energies of 1.46 and 1.63 eV respectively. For the case of WSe_2, the valence band maximum (VBM) is seen to cross the Fermi level only in the band structure. Further work for each investigation is suggested to resolve discrepancies in the results via an examination of the simulation procedure and additional analysis.

Introduction

Computational methods are employed in materials science to explore material properties and behaviour to a finer level of detail and in more complex scenarios than is possible through pure theory and experimentation. Two main streams of computational (simulation) methods exist which serve to explore different domains of materials science research. The first group are Molecular Dynamics (MD) methods, which integrate the positions and velocities of a set of interacting particles by numerically solving Newton's equations of motion. Interatomic potentials (known as "force fields") determine the forces and potential energies between particles at each timestep, and simulations typically involve 100's-1000's of particles. MD thus allows for the evolution of dynamical, macroscopic properties of a system to be studied under different conditions. The second set are known as *ab initio* (from first principles) quantum mechanical (QM) methods. These simulations perform static calculations (i.e. no time evolution) to determine the quantum behaviour of a system by solving the Time Independent Schrodinger Equation (TISE) through various approximations. Most commonly used is the Kohn-Sham formalism of Density Functional Theory,[1] which parameterises the electron density and reduces the many-body TISE to a problem of non-interacting electrons moving in an effective potential. Calculations are typically limited to systems involving 10's-100's of atoms due to intensive computational requirements and allow for the determination of fundamental electronic properties such as the ground state energy, density of states (DOS) and band structure.

In the following investigation, MD and QM simulations are performed independently for different chemical systems to demonstrate their separate usage. First, the thermal conductivity of a Single Wall Carbon Nanotube (SWCNT) is determined via a set of MD simulations with respect to varying temperature. The lattice constant of the graphene honeycomb lattice of the SWCNT is $a = 2.49$ Å, whilst the CNT itself is setup in an armchair configuration with chiral indices $m = 10$ and $n = 10$, as shown in Fig. 1. Further, the length of the SWCNT is chosen to be 440 Å, which ensures a minimum length/diameter ratio of 10. Finally, the

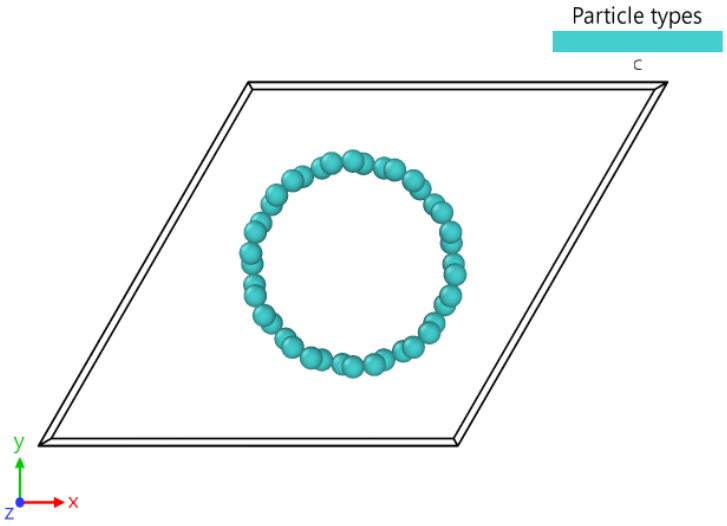

Figure 1: Top-down view of a Single Wall Carbon Nanotube (SWCNT) with chiral indices $m = 10$ and $n = 10$ (an armchair configuration), generated using the Ovito software package.[2]

DOS and band structure of monolayer Molybdenum Disulfide ($MoSe_2$) and Tungsten Disulfide (WSe_2) are calculated through QM DFT simulations. Each structure crystallises in the $P\bar{6}m2$ space group, and the structure is displayed in Fig. 2.

Computational Details

To model the atomic interactions and time evolution of the SWCNT through classical mechanics we make use of the Large-scale Atomic/Molecular Massively Parallel Simulator (LAMMPS).[4] The MD simulations use the Tersoff bond order potential,[5] utilising modified parameters optimised for thermal transport calculations.[6] The positions and velocities of each carbon atom are integrated using the Verlet algorithm, which solves Newton's equations of motion. A fixed timestep for the integration of 0.001 fs was chosen, and the simulation cell is defined to span an orthogonal box in (x, y, z) from (-50, -50, 0) to (50, 50, 440) Å.

In order to simulate heat flow between hot and cold regions, the SWCNT is divided into twenty segments and a temperature gradient is imposed by fixing two Langevin thermostats at two positions in the tube. The right-most end of the nanotube is connected to a "hot"

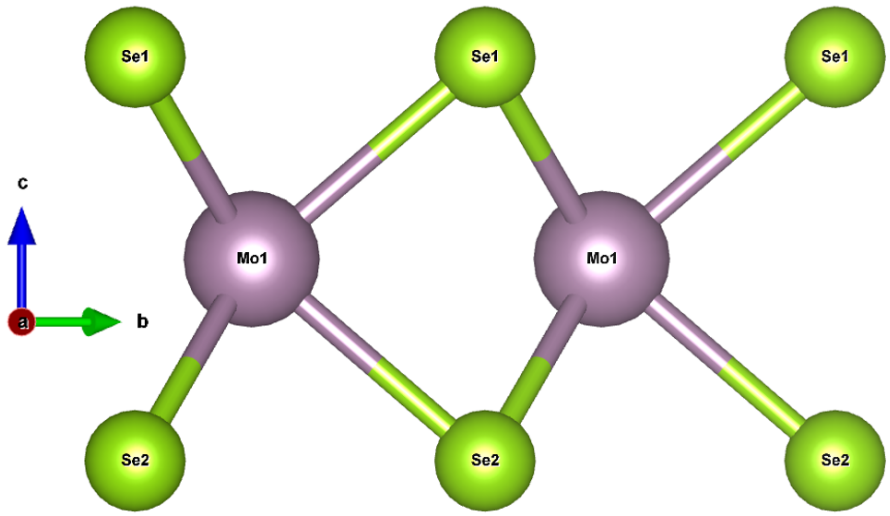

Figure 2: Side-view of monolayer $MoSe_2$, with the unit cell replicated in the b axis. The structure of WSe_2 is essentially identical (lattice constant and length of crystal axes aside), except the W atoms are substituted for Mo. Diagram generated using VESTA.[3]

bath, whilst the middle segment is attached to a "cold" bath, which allows the use of a periodic boundary condition along the nanotube axis. This experimental setup is similar to that used in a comparable study into the thermal conductivity of SWCNTs for varying chiral index with respect to temperature.[7] At equilibrium this setup simulates a thermal gradient sustained by the exchange of energy between hot and cold regions of the SWCNT. The thermal conductivity, κ, is calculated during the simulation using the following formula:

$$\kappa = \frac{Qd}{A\Delta T} \tag{1}$$

where Q is the total heat transferred to/from the system by the thermostats to maintain the temperature gradient, d is the distance between the isothermal planes, A is the surface area of the isothermal planes and ΔT is the temperature gradient.

To solve the many-atom, many-electron Schrodinger Equation within the framework of Density Functional Theory (DFT) we make use of the Abinit software package,[8,9] which provides the capability to evaluate and optimise the total energy and electronic structure

of molecules and periodic (crystalline) materials. The norm conserving (NC) pseudopotential approach[10] is selected to describe the fundamental atomic-scale interactions, whilst the Perdew-Burke Ernzerhof (PBE) generalized gradiant approximation (GGA) is utilised to account for the exchange-correlation energy.[11] A standard convergence study was performed to determine the most stable parametrisation of the system for MoSe2 with a stopping criterion of $\Delta E = 1 \times 10^{-6}$ eV, and is shown in Fig. 3. Consequently, a cutoff energy of 35 Ha was chosen for the plane-wave basis set, along with a (5x5x1) k-point mesh to sample the Brillouin Zone (BZ) via the Monkhorst-Pack method[12] during geometric relaxation. Finally, the high symmetry path used to construct the band structure of the monolayer, hexagonal unit cells in the Brillouin Zone are built in accordance with standard techniques.[13]

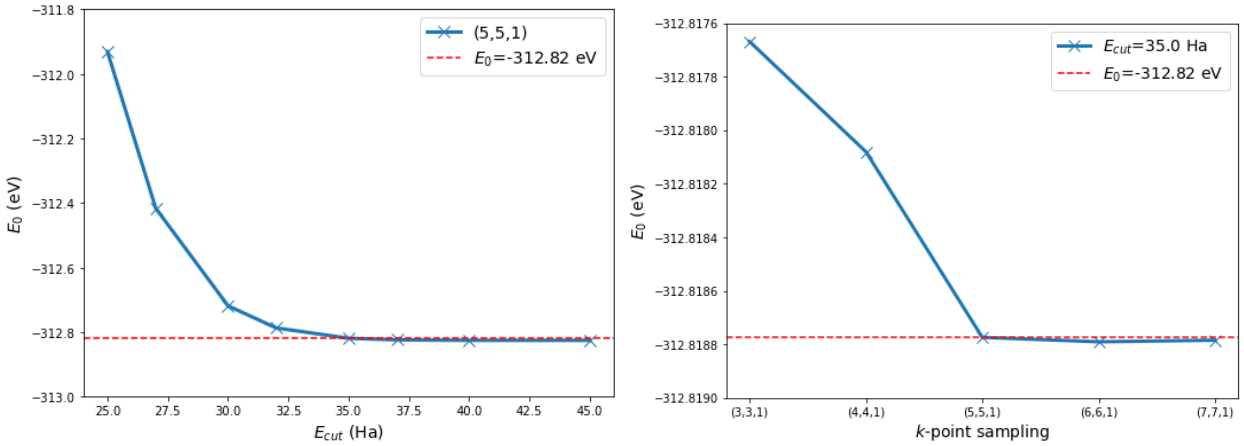

(a) ECUT (b) KPTS

Figure 3: Demonstration of convergence in ground state energy (E_0) when varying the input parameters for a) the plane wave cutoff energy (ECUT) and b) the k-point grid (KPTS).

Results

The outcome of the MD investigation for the (10,10) armchair SWCNT with respect to varying temperature is shown in Fig. 4. The results show that the thermal conductivity, κ, grows linearly with temperature reaching a peak value at 500K of 3340W/mK, with a gradient of 6.4 W/mK^2. The trend observed in this data is in disagreement with another

existing study for (10,10) SWCNTs,[7] where the value of κ is seen to peak at 400K at around 2750 W/mK before dropping off at 500K. Furthermore, the increase in κ up to 400K is non-linear. A different study found the value of the thermal conductivity to be $\kappa = 6600$ W/mK at room temperature, whilst peaking at 100K.[14] Thus, the values observed for κ are on the correct order of magnitude, but the simulations do not predict the expected non-linear behaviour and peak in thermal conductivity over a temperature range between 100-500 K, as observed in the studies referenced above. The cause of the divergent behaviour of the results observed in these simulations is unknown. Additional tests were run with different chirality, tube length and over greater temperature ranges to attempt to observe if this behaviour is replicated or merely an anomaly. However, these tests did not produce any meaningful results. At lower chirality (only in an armchair configuration, examples tested were 5,5 and 8,8), thermal equilibrium could not be reached (the temperature grew exponentially) despite adjusting the length of the CNT to maintain the L/d ratio greater than 10. Consequently, further detailed analysis is required in order to determine the root cause of these issues. This would likely involve testing at higher chirality (e.g. 12,12; 15,15 ...) to see if the results are an anomaly. If so, it is likely that there are issues caused by the simulation procedure, which should be revisited and improved.

When running the QM simulations for both $MoSe_2$ and WSe_2, a geometric relaxation was first performed to minimise the forces acting between the atoms, with the lattice constant given in Table 1. Following this, the electronic density of states (DOS) and band structure were determined for each system and are shown in Figs. 5 and 6 (DOS plots), and Figs. 7 and 8 (band structure plots) respectively. Key electronic properties of each material are also reported in Table 1. Note that each plot is shifted in their respective axes such that the Fermi level lies at 0 eV for consistency. Further, the total electronic density of states (TDOS) as given in Figs. 5 and 6 is only the sum of the partial density of states (PDOS), as opposed to the full density of states of each material. The partial value is reported since analysis of the DOS is limited to an investigation of which type of atom is contributing to

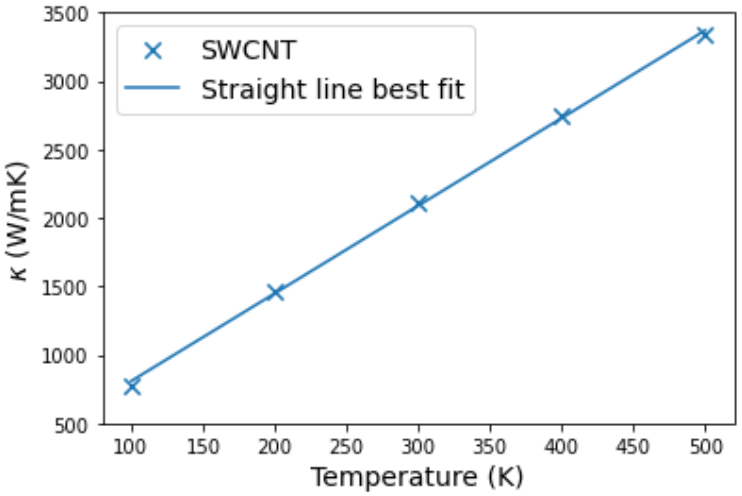

Figure 4: Thermal conductivity (κ) versus temperature of a Single Wall Carbon Nanotube (SWCNT). A straight line of the form $y = mx + c$ is fitted to the data, with $m = 6.40$ W/mK^2 and $c = 128$ W/mK.

the valence band maximum (VBM) and conduction band minimum (CBM).

Table 1: Structural and electronic properties of $MoSe_2$ and WSe_2 including: lattice parameter, a (Å); fermi energy, E_F (eV); band gap energy, E_{gap} (eV); valence band maximum, E_{VM} (ev) and the conduction band maximum, E_{CM} (eV). All values are quoted to three significant figures.

Structural and Electronic Properties	**$MoSe_2$**	**WSe_2**
a	3.32	3.32
E_F	-0.122	-0.788
E_{gap}	1.46	1.63
E_{VM}	-0.685	0.0280
E_{CM}	0.771	1.60

We report $MoSe_2$ as a direct band gap semiconductor with a band gap energy of $E_{gap} = 1.46$ eV. It is well known that monolayer MX_2 materials (M=metal, X=chalcogen) exhibit a direct band gap at 0K, and the value of the band gap energy and its location (at the K high-symmetry point) is in agreement with literature for other PBE-GGA based calculations.[15] Further, the main contributions to the VBM and CBM come from the Mo atom.

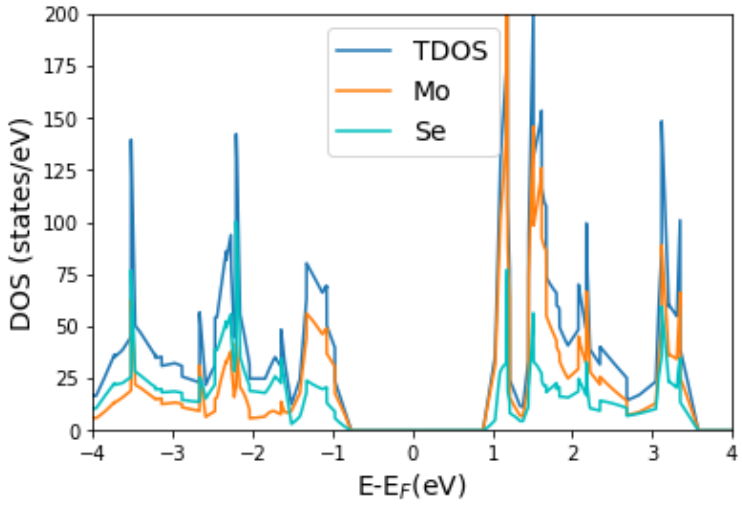

Figure 5: MoSe2 density of states (DOS). TDOS represents the total projected DOS of all atoms, whilst curves belonging to Mo and Se represent the contribution to the DOS from each atom type.

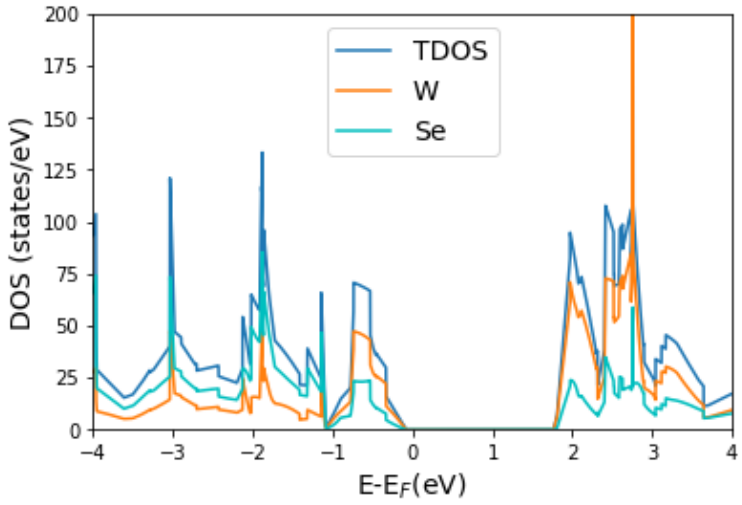

Figure 6: WSe2 density of states (DOS). TDOS represents the total projected DOS of all atoms, whilst curves belonging to W and Se represent the contribution to the DOS from atoms of each type.

Similarly, WSe_2 is found to be a direct band gap semiconductor with a band gap energy of $E_{\text{gap}} = 1.63$ eV. The direct characteristic of this band gap is again in agreement with literature, although value of the band gap energy is slightly larger than reported in literature.[15] Again, the main contributions to the VBM and CBM arise from the Mo atom. However, the results between the DOS (Fig. 6) and band structure (Fig. 8) are in slight disagreement. It

is observed that the edge of the valence band (i.e. the VBM) crosses the Fermi level in the band structure plot, whereas it lies slightly below in the DOS. The cause of this problem is unknown, and further investigation of the simulation parameters should be performed to understand the cause of the discrepancy.

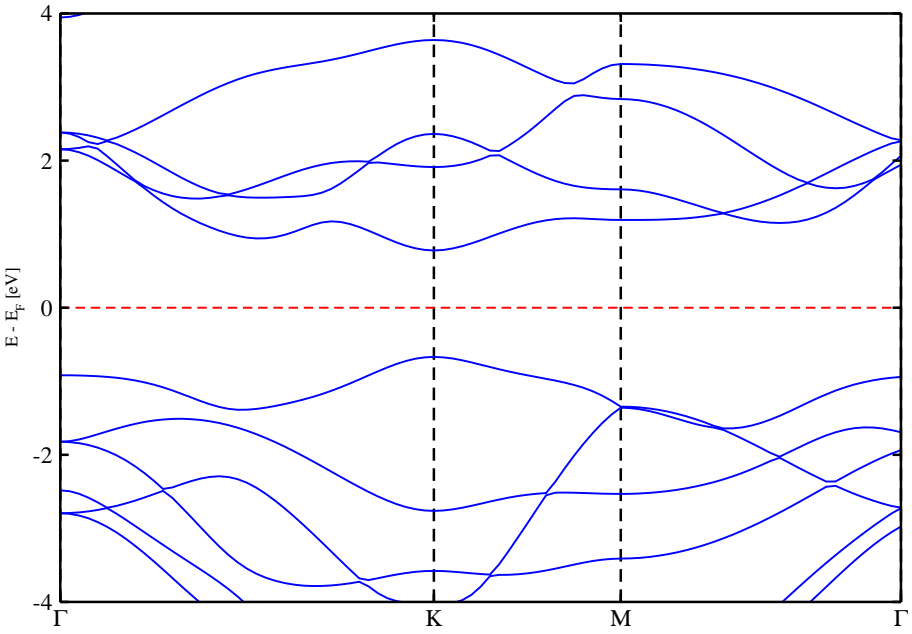

Figure 7: MoSe2 band structure following high symmetry path Γ-K-M-Γ. A direct band gap is observed at the K high symmetry point with a value of 1.46 eV.

Interestingly, it can be seen from Figs. 7 and 8 that for $MoSe_2$, the VBM lies below the Fermi level whereas for WSe_2, it lies above. This might lead to a lower relative stability of WSe_2 compared to $MoSe_2$, since it allows for enhanced electronic interactions. However, this insight would need to be confirmed by further analysis of the stability of the two materials. Moreover, the level of analysis performed here is surface level, and further work would need to be performed to examine the exact contributions of the different atomic orbitals at the valence and conduction band edges.

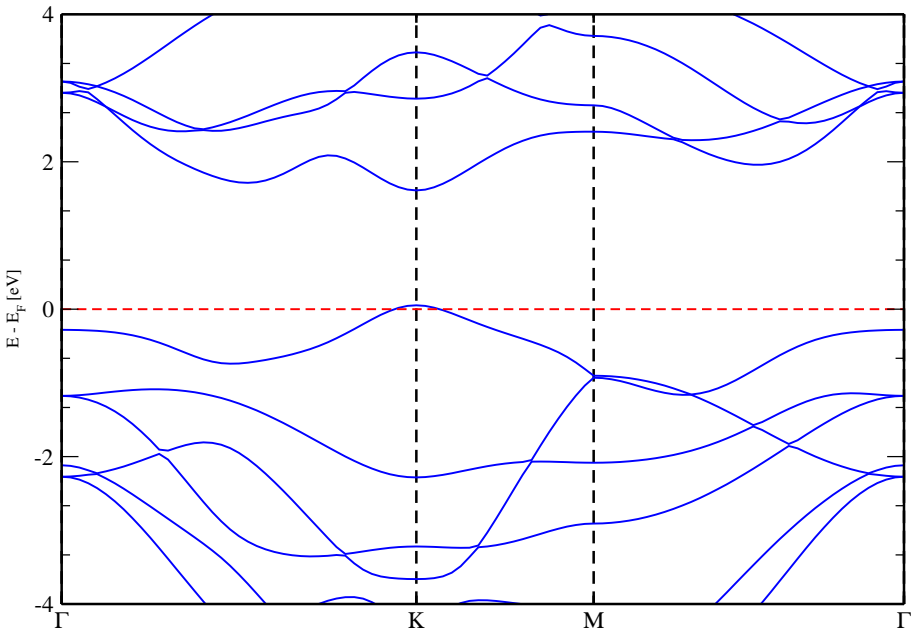

Figure 8: WSe2 band structure. WSe2 band structure following high symmetry path Γ-K-M-Γ. A direct band gap is observed at the K high symmetry point with a value of 1.63 eV. The edge of the valence band is seen here to cross the Fermi level, allowing for enhanced electronic interactions with respect to $MoSe_2$.

Conclusion

Through a molecular dynamics (MD) simulation of a Single Wall Carbon Nanotube (SWCNT) with chirality (10,10), the thermal conductivity κ was measured with respect to temperature betwen 100-500 K. The individual values measured for κ in the temperature range studied are within the same order of magnitude as those reported previously in literature.[7] However, the thermal conductivity was found to be growing linearly with respect to temperature with gradient $m = 6.40$ W/mK. This is in disagreement with the general behaviour observed for κ, where its value peaks at a certain (variable) temperature between 100-500 K before dropping off again. It is noted that during the simulation procedure, difficulty was encountered in ensuring the system reached a stable thermal gradient and this could be a cause for the problem as outlined above. Further work should be performed to examine the simulation procedure to test if this result is only an anomaly.

The second set of simulations involved performing first principles / quantum mechanical (QM) simulations to determine the electronic density of states (DOS) and band structure of $MoSe_2$ and WSe_2. Each material is found to be a direct band gap semiconductor with a band gap energy of 1.46 and 1.63 eV respectively, broadly in agreement with existing literature. Further, the largest contributions to the valence band maximum (VBM) and conduction band minimum (CBM) in both cases arise from the Mo atom. A more comprehensive study of the main electron orbitals which contribute to the VBM and CBM was not performed here. Interestingly, it is seen that the VBM for WSe_2 crosses the Fermi level. The material is therefore more conductive and thus likely to be less stable, however the relative stability was not investigated in this study and is a topic for future work.

To conclude, the initial aims of this study were to demonstrate the different functions and purposes of MD and QM simulations. Generally speaking, this has been achieved. However, significant issues are present in the measurement of the thermal conductivity of the SWCNT which would need to be addressed in future work, and more detailed investigation should be performed on the electronic structure of $MoSe_2$ and WSe_2.

References

(1) Kohn, W.; Sham, L. J. Self-Consistent Equations Including Exchange and Correlation Effects. *Phys. Rev.* **1965**, *140*, A1133–A1138.

(2) Stukowski, A. Visualization and analysis of atomistic simulation data with OVITO-the Open Visualization Tool. *MODELLING AND SIMULATION IN MATERIALS SCIENCE AND ENGINEERING* **2010**, *18*.

(3) Momma, K.; Izumi, F. *VESTA3* for three-dimensional visualization of crystal, volumetric and morphology data. *Journal of Applied Crystallography* **2011**, *44*, 1272–1276.

(4) Thompson, A. P.; Aktulga, H. M.; Berger, R.; Bolintineanu, D. S.; Brown, W. M.;

Crozier, P. S.; Kohlmeyer, A.; Moore, S. G.; Nguyen, T. D.; Shan, R.; Stevens, M. J.; Tranchida, J.; Trott, C.; Plimpton, S. J. LAMMPS - a flexible simulation tool for particle-based materials modeling at the atomic, meso, and continuum scales. *Comp. Phys. Comm.* **2022**, *271*, 108171.

(5) Tersoff, J. New empirical approach for the structure and energy of covalent systems. *Phys. Rev. B* **1988**, *37*, 6991–7000.

(6) Lindsay, L.; Broido, D. A. Optimized Tersoff and Brenner empirical potential parameters for lattice dynamics and phonon thermal transport in carbon nanotubes and graphene. *Phys. Rev. B* **2010**, *81*, 205441.

(7) Osman, M. A.; Srivastava, D. Temperature dependence of the thermal conductivity of single-wall carbon nanotubes. *Nanotechnology* **2001**, *12*, 21.

(8) Gonze, X. et al. The Abinit project: Impact, environment and recent developments. *Comput. Phys. Commun.* **2020**, *248*, 107042.

(9) Romero, A. H. et al. ABINIT: Overview, and focus on selected capabilities. *J. Chem. Phys.* **2020**, *152*, 124102.

(10) Hamann, D. R.; Schlüter, M.; Chiang, C. Norm-Conserving Pseudopotentials. *Phys. Rev. Lett.* **1979**, *43*, 1494–1497.

(11) Perdew, J. P.; Burke, K.; Ernzerhof, M. Generalized Gradient Approximation Made Simple. *Phys. Rev. Lett.* **1996**, *77*, 3865–3868.

(12) Monkhorst, H. J.; Pack, J. D. Special points for Brillouin-zone integrations. *Phys. Rev. B* **1976**, *13*, 5188–5192.

(13) Setyawan, W.; Curtarolo, S. High-throughput electronic band structure calculations: Challenges and tools. *Computational Materials Science* **2010**, *49*, 299–312.

(14) Berber, S.; Kwon, Y.-K.; Tománek, D. Unusually High Thermal Conductivity of Carbon Nanotubes. *Phys. Rev. Lett.* **2000**, *84*, 4613–4616.

(15) Chang, C.-H.; Fan, X.; Lin, S.-H.; Kuo, J.-L. Orbital analysis of electronic structure and phonon dispersion in MoS_2, $MoSe_2$, WS_2, and WSe_2 monolayers under strain. *Phys. Rev. B* **2013**, *88*, 195420.